Chemical Physics Letters 796 (2022) 139569

Contents lists available at ScienceDirect

Chemical Physics Letters

journal homepage: www.elsevier.com/locate/cplett

Hydrothermal synthesis of undoped and inner transition metals (neodymium (Nd), gadolinium (Gd)) doped tin monosulfide (SnS) nanostructures: Comparative study of the morphological, opto-magnetic properties and antibacterial performance

J. Gajendiran [a,*], S. Gnanam [b,*], V.P. Senthil [c], J. Ramana Ramya [d], K. Ramachandran [e], V. Vijayakumar [f], S. Gokul Raj [g], G. Ramesh Kumar [h], N. Sivakumar [i]

[a] Department of Physics, Vel Tech Rangarajan Dr.Sagunthala R&D Institute of Science and Technology, Avadi, Chennai 600 062, India
[b] Department of Physics, School of Basic Sciences, Vels Institute of Science, Technology & Advanced Studies (VISTAS), Pallavaram, Chennai 600 117, India
[c] Senior Staff Officer (Education), HQ WNC, Mumbai 400005, India
[d] National Center for Nanoscience and Nanotechnology, University of Madras, Chennai 60 0 025, Tamilnadu, India
[e] Department of Physics, SRMIST, Vadapalani Campus, Chennai 600026, India
[f] Department of Chemistry, Karan Arts and Science College (Co-Ed), Thenmathur, Tiruvannmalai 606603, India
[g] Department of Physics, C. Kandaswami Naidu College for Men, Annanagar, Chennai 600102, India
[h] Department of Science and Humanities, University College of Engineering Arni, Anna University Chennai, Thatchur, Arni 632 326, India
[i] Sri Sai Ram Engineering College, West Tambaram, Chennai 600044, India

ARTICLE INFO

Keywords:
Metal sulfide
Hydrothermal synthesis
Optical properties
Magnetic properties
Antibacterial activity

ABSTRACT

Undoped SnS, and Nd and Gd-doped SnS nanostructures were fabricated by hydrothermal approach. The XRD study for the Gd-doped SnS powder proved the formation of an orthrhombic crystal structure. The SEM study reveals the particles' surface altered by introducing the Nd and Gd element into the SnS materials. Undoped and doped SnS materials have ferromagnetic characters detected, along with the distinct coercive force and intense magnetization revealed by VSM study. Significantly reduced band gap values have been observed for doped SnS in the optical absorption spectra. The antibacterial activity of prepared materials was tested, and the results have been discussed in detail.

1. Introduction

Tin monosulfide (SnS) is one of the chalcogenide materials which has turned research topic and gained much attention for use in industrial applications, in photo detectors (photodiodes and photovoltaic) as optoelectronic devices, waste water treatment &biomedical, solar cells, gas sensors etc. [1–5]. From the available past and recent literature reports, some merits were noticed about SnS material, like narrow optical band gap energy, infrared (IR) and near-infrared (NIR) optical behaviour, non-toxicity, good light-absorption and transparency, and moderate electrical resistivity and conductivity.

A lot of web reports deal with the synthesis of metals (In, Fe, Ti, V, Se, Sb, Te, Cu, Na), non- metals (Carbon, Nitrogen, Phosphorus), reduced graphene oxide and g-C_3N_4 doped SnS material by different chemical routes for testing the optical, electronic, magnetic properties, electrical and thermoelectric behaviour when used in optoelectronic devices, solar cells, waste water treatment, electrochemical, gas sensing and spintronics device applications [6–27]. For example, Pandey et al. [28] synthesized the undoped and various concentrations of Mn doped SnS nanoparticles through the chemical precipitation method. They found significant changes in the optical band gap and photoemission characteristic with respect to increasing the Mn dopant concentration on the SnS nanoparticles. Arepalli et al. [29] tested the concentration of 2%- Ag doped SnS thin film materials at various temperatures (200 to 350 °C) via the sputtering method. They examined the surface modification of the morphologies, crystalline behaviour, interplanar distance, Full width half maximum, intrinsic strain, lattice constant, cell volume, composition of elements, optical and electrical parameters under the influence of temperatures ranging from 200 to 350 °C. Jethwa et al. [30] made Se dopant admixtures in a SnS crystal by the direct vapour

* Corresponding authors.
E-mail addresses: gaja.nanotech@gmail.com (J. Gajendiran), gnanam.physics@gmail.com (S. Gnanam).

https://doi.org/10.1016/j.cplett.2022.139569
Received 22 December 2021; Received in revised form 1 March 2022; Accepted 14 March 2022
Available online 16 March 2022

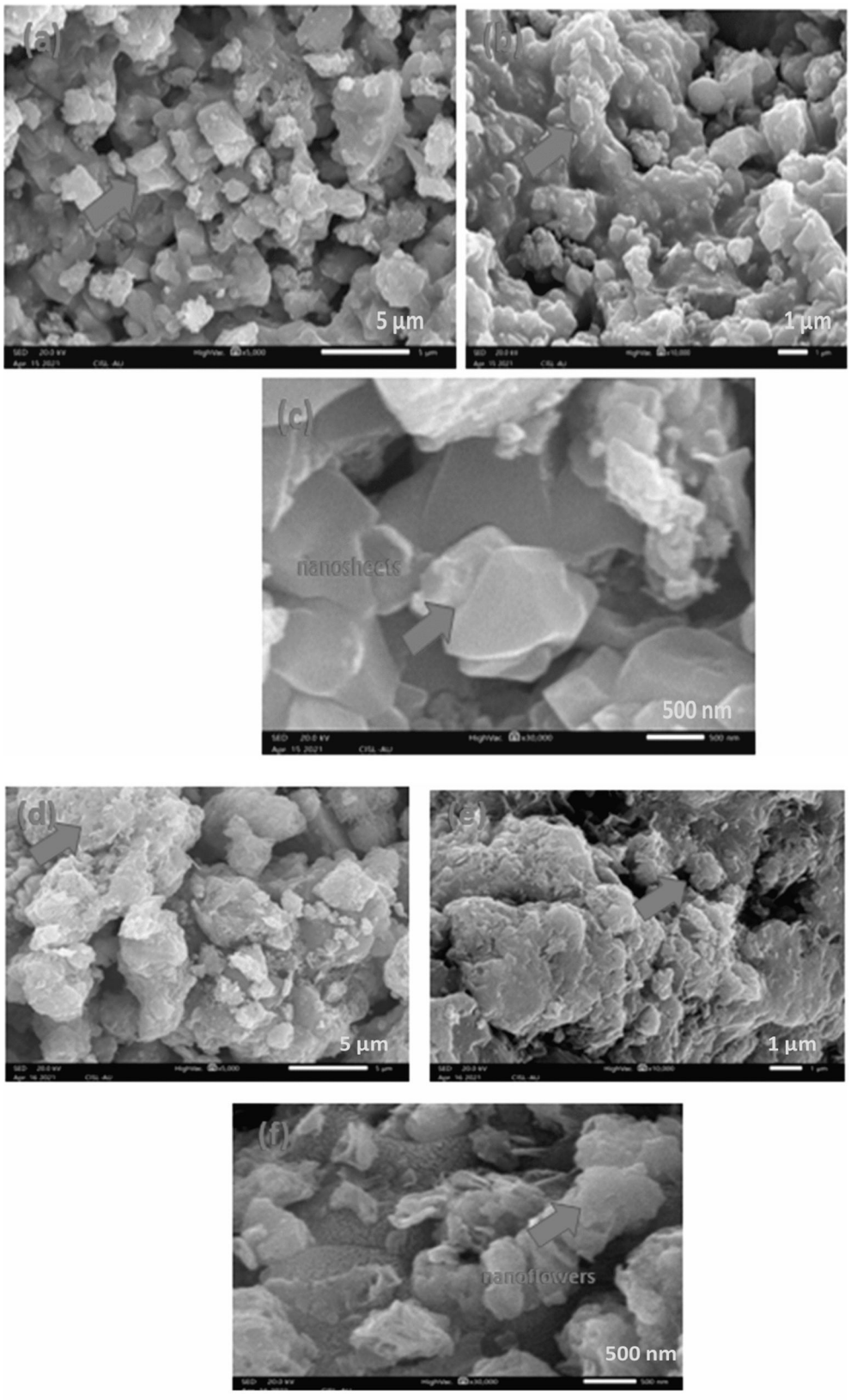

Fig. 1. Different magnification images of (a-c) undoped SnS, (d-f) Nd-doped SnS, (g-i) Gd-doped SnS nanostructures and (j) schematic formation mechanism of the Gd-doped SnS material.

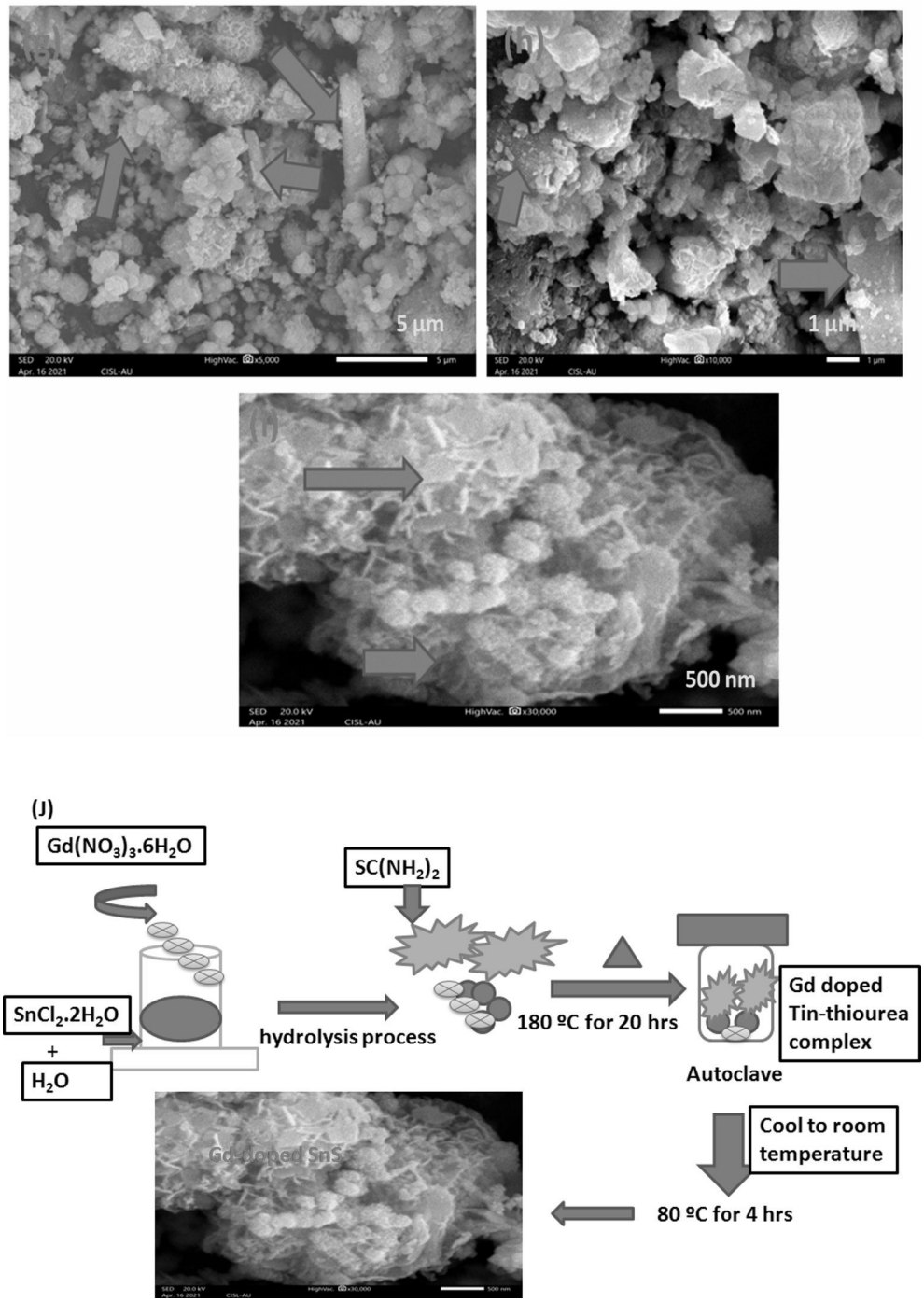

Fig. 1. (*continued*).

transport route. They found improved electrical responses like the hall coefficient, conductivity, mobility and carrier concentration and photodetector parameters in the Se doped SnS crystal. Purusottam Reddy Bommireddy and his groups [31] investigated the tuning of diffraction shifts, the Raman shift from the XRD and Raman spectra, surface modification, elemental composition ratio, optical band gap and electrical parameters (carriers' concentration, mobility, resisitivity, material type (p-n-type)) by introducing various concentrations of a copper dopant incorporated in the SnS thin film material via the spin coating route. Qin et al. [32] prepared an Ag doped SnS thin film using the solvo-thermal method followed by a study of the gas sensing characteristic. In this paper, the obtained gas sensing parameters of the Ag doped SnS film are compared with the computation theory based gas sensing parameters' results and discussed in detail. Janakiraman et al. reported [33] that undoped and Fe doped SnS thin films were deposited on the glass substrate by applying certain parameter conditions via the spray coating analysis. In this paper, they found that the average crystallite size was decreased in the SnS film material with increasing Fe doped concentration. Variation in the surface modifications were noticed in the microscopy studies by varying the Fe doped concentration admixtures in the SnS film. In addition, better optical absorbance and transmittance were found in Fe doepd SnS film at higher concentration in the optical spectra studies. Using co-precipitation, Parveen et al. [34] studied the undoped and different concentrations of Ni dopant assisted SnS nanocrystalline materials. They noticed that tuning affected the average crystallite size and physical properties like the lattice constant,

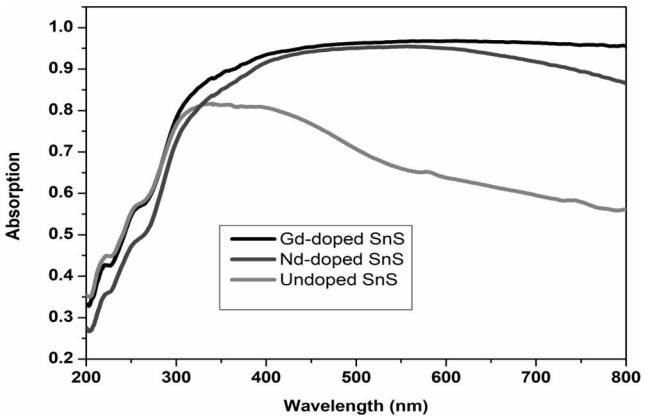

Fig. 2a. UV visible spectra of (a) undoped SnS, (b) Nd doped SnS and Gd-doped SnS material. b Tauc plot of (a) undoped SnS, (b) Nd doped SnS and Gd-doped SnS material.

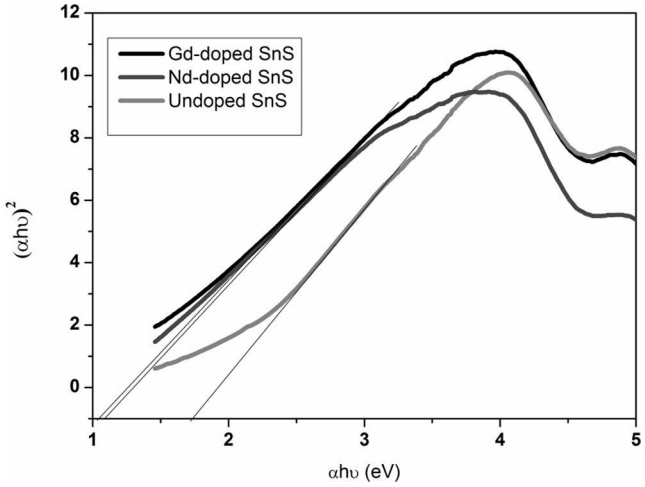

Fig. 2b. Tauc plot of (a) undoped SnS, (b) Nd doped SnS and Gd-doped SnS material.

crystalline strain, dislocation density, volume of the unit cell and internal surface modification and electrical characteristics (dielectrics and conductivity) under the influence of Ni dopant concentration in the SnS material. Muthalif et al. [35] reported the better electrochemical and photovoltaic activity of Cu doped SnS compared to the pure SnS material through the chemical bath deposition method. In addition, they noticed that improved photovoltaic behaviour of Cu doped SnS is suitable for solar cells applications. Ag doped SnS thin film was prepared using the spray route and the effects of the Ag dopant concentration on the optical band gap, and structural and electrical parameters values were comparatively discussed in detail by Santhosh Kumar and his groups [36]. Structural, optical absorption, emission behaviour and electrical properties of the co-precipitation synthesized pure and Pb doped SnS material were comparatively examined by Mohammad Reza Arefi-Rad et al. [37]. They noticed improved physico-chemical properties in the Pb doped SnS material. Based on the above literatures, it was noticed that on introducing the above dopants into the SnS material, the structural parameter results like the crystallite size, strain, and topographical particles etc. could be tuned. In addition, for the doped SnS material, an increase or decrease in the optical band gap and emission band peaks, depends on selecting the dopant material [6,7, 13–16, 27, 31, 33]. This happened due to the ionic radius variation between the dopant and tin ions. The optical band gap value is one of the reasons affecting the catalytic activity [2]. If the optical band gap values and PL emission intensity are decreased their consequences will generate more recombinations of electron-hole pairs. Thus, the optical property would enhance the catalytic activity of the nanomaterial. Moreover, improved coercivity and magnetization values of the SnS material by increasing the dopant concentrations were detected from the magnetization–applied field (M−H) curve, compared with the pure SnS compound [10,34]. This was because of the interaction between the dopant ions and tin ions, when a magnetic field is applied on the doped SnS material.

The SnS material with the above dopants incorporated into was synthesized by applying different chemical routes. The hydrothermal route was used to synthesize the undoped, and Gd and Nd-doped SnS material. From the above literature reports it was noticed that, the hydrothermal route has some merits it could be used without any surfactants/inert gas for a high temperature reaction compared to the other chemical techniques [38–45].

The present investigation, attempts to study undoped SnS, and Nd and Gd-doped SnS bioceramic nanopowders by taking tin (II) chloride salt, thiourea, water, gadolinium nitrate and neodymium nitrate salt used as a doping agent through the hydrothermal method. The synthesized undoped and doped SnS nanostructures were tested by various sophisticated analytical instruments such as UV–visible spectroscopy, Vibrating Sample Magnetometer (VSM), and the antibacterial studies and their results are discussed detail for the first time. In addition, it was found that the Gd doped SnS nanostructures has good optical and magnetic properties and antibacterial activity compared to the undoped and Nd-doped SnS compound. Hence, the powder X-ray powder diffraction (XRD) pattern for the Gd doped SnS material was examined with respect to its crystalline structure and its discussion is presented in detail.

2. Experimental

2.1. Synthesis of Undoped, Nd-and Gd- doped SnS material

Synthesis chemicals of the analytical grade have been used without further purification to obtain undoped, Nd-and Gd-doped SnS material using the hydrothermal route. 0.1 mmol of tin (II) chloride di hydrate ($SnCl_2{\cdot}2H_2O$, Sigma-Aldrich-purity 99.9%) was taken as a tin precursor and dispersed in 80 mL quantity of distilled water. Now, the tin precursor salt was slowly dissociated into the distilled water, forming tin and chlorine ions separately due to the hydrolysis process. In the next step, 0.01 mmol of gadolinium (III) nitrate hexa hydrate ($Gd(NO_3)_3{\cdot}6H_2O$, Sigma-Aldrich-purity 99.9%) salt was taken as a dopant and dispersed into the above solution. After that, 0.1 mmol of thiourea salt ($SC(NH_2)_2$, Sigma-Aldrich purity 99%) was taken as a sulfur source and added to the aqueous Gd doped tin solution under magnetic stirring for a few minutes to form the tin-thiourea complex. The above solution was transferred to a stainless steel autocalave and the reaction temperature was fixed at 180 °C for 20 hrs. The obtained product was taken out and allowed to cool at room temperature and washed with ethanol followed by water several times and filtered using Whattman paper. The filtered precipitate was kept at 80 °C for 4 hrs to obtain the Gd-doped SnS powder. Similarly, Nd doped SnS powder was fabricated by taking tin tetra chloride pentahydrate, distilled water, thiourea and Neodymium nitrate (Sigma-Aldrich purity 99.9%) using the solvothermal method. In addition, undoped SnS material was also prepared using tin (II) chloride dihydrate, distilled water and thiourea.

2.2. Characterization

Topographical structures were identified with the aid of Scanning Electron Microscopy (JEOL; JSM-67001 SEM). Using UV–Visible spectra (Jasco V-760 UV–visible spectrometer instrument) to scan the optical absorption data of the synthesized products, their optical band gap values were examined. Vibrating Sample Magnetometer (Lakeshore

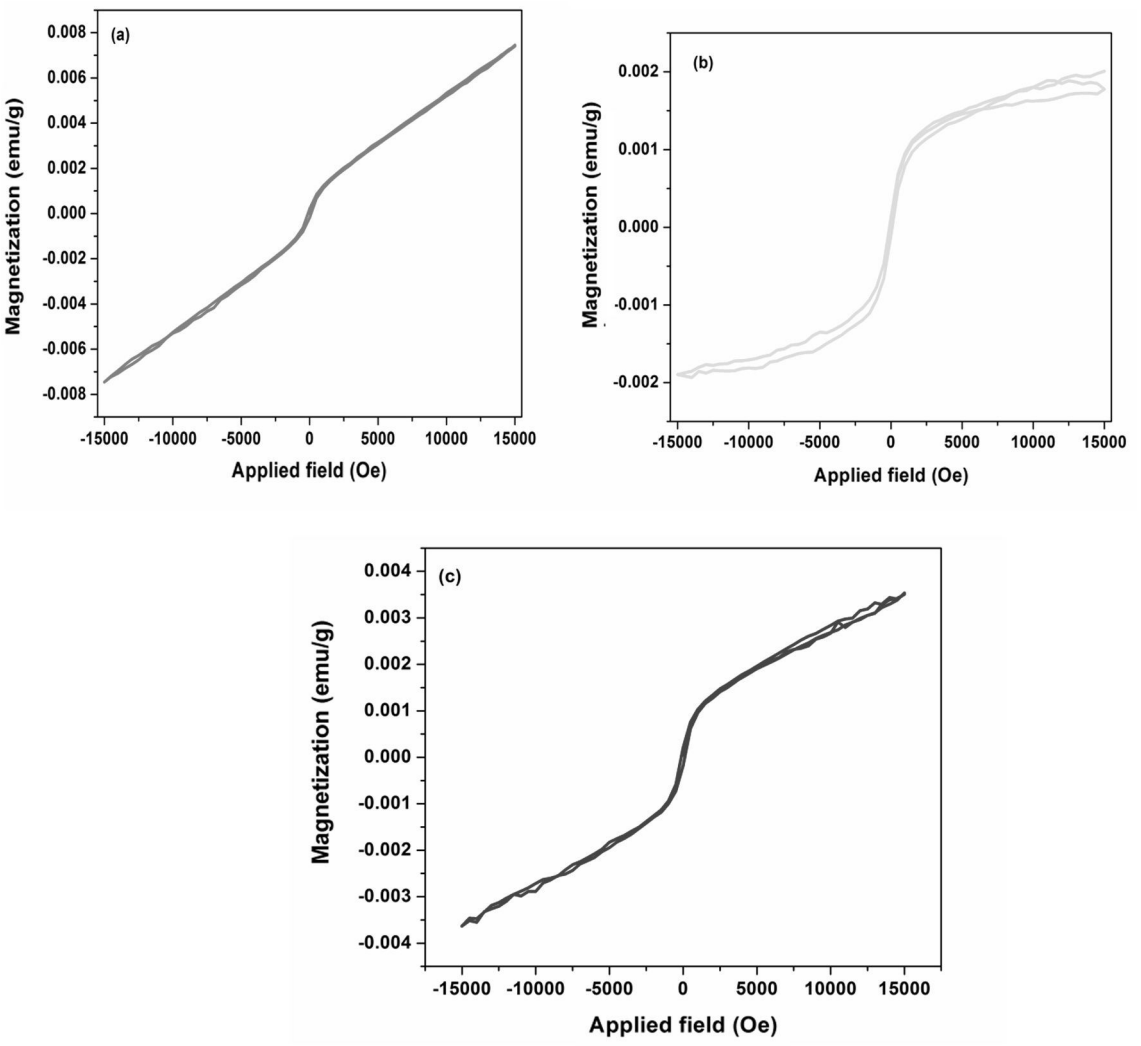

Fig. 3. M-H curve of (a) undoped SnS, (b) Nd doped SnS and (c) Gd doped SnS samples.

Table 1
Comparative study of magnetic nature and coercivity values of undoped, and doped SnS material.

Material	Coercivity (Hc) (Oe)	Magnetic nature
Undoped-SnS	120.45	Weak ferromagnetism
Nd-doped SnS	96	Weak ferromagnetism
Gd-doped SnS	122	Weak ferromagnetism

VSM model 740) was run in the applied magnetic field range as −15,500 to 15,500 Oe. The synthesized Gd-doped SnS sample were tested on a powder X-Ray Diffraction (X'pert PRO powder XRD instrument) to scan their diffraction peaks and their angles in the range between 10 and 70° by applying a wavelength ($\lambda = 1.540$ Å) of Cuk$_\alpha$ radiation.

2.3. Antimicrobial activity

The antibacterial competence of the undoped SnS, Nd doped SnS and Gd doped SnS was studied against E. Coli (gram-negative strain) by the agar plate diffusion technique [3,46–50]. The nutrient agar of 28 g was dispersed in 1000 mL distilled water and boiled at 15 psi for 20 min. The plates were cast with 25 mL of the agar solution and allowed to cool. The bacterial suspension of 30 μL was spread over the plates uniformly and wells were made in the plates. 5 mg/mL samples were dispersed in triple distilled water and added in the well. Then the plates were kept at 37 °C

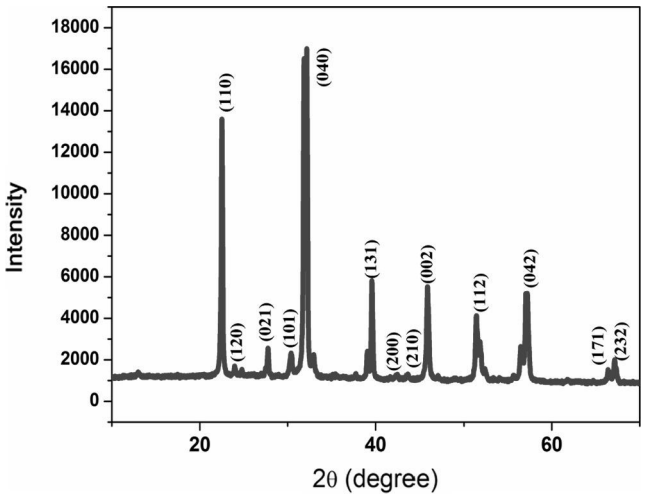

Fig. 4. XRD pattern of the Gd-doped SnS material.

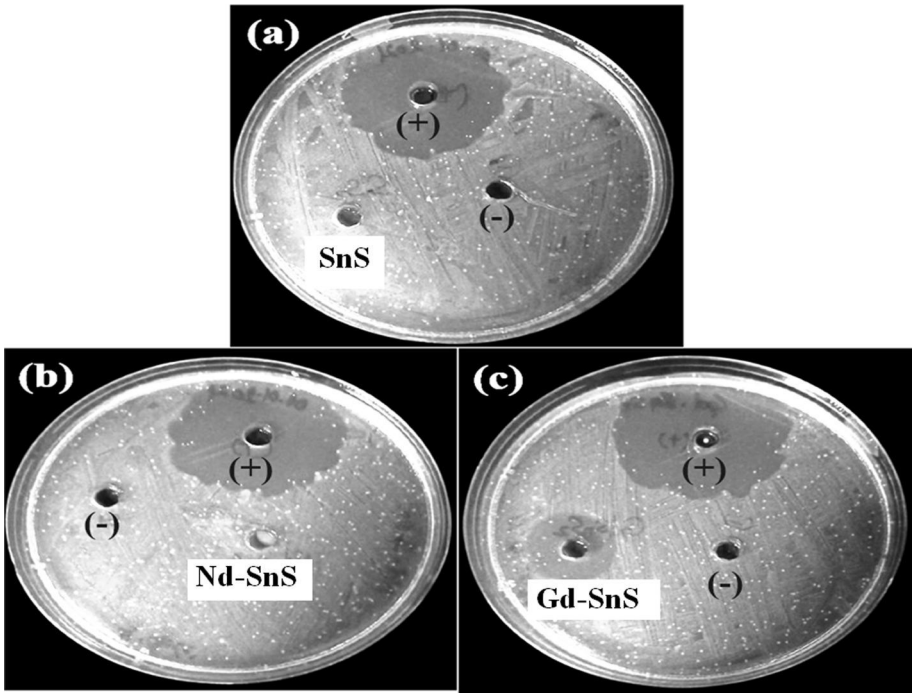

Fig. 5. Antibacterial activities of (a) SnS, (b) Nd-SnS and (c) Gd-SnS against the gram-negative strain *E. coli*.

for a day and the zone of inhibition was measured and photographed. The experiments were repeated in triplicate.

3. Results and discussion

Different magnification images of the (a-c) undoped SnS, (d-f) Nd-doped SnS and (f-h) Gd-doped SnS materials are shown in Fig. 1. In the SEM images, the nanostructured formation of particles the synthesized undoped and doped SnS material could be clearly seen nanosheets, nanoflowers and nanosheets/rods along with spherical particle morphology was seen for the undoped SnS, Nd-doped SnS and Gd-SnS materials. It was noticed from the SEM results, that the introduction of the dopant plays a significant role in changing change the surface modification of the particles. A schematic formation mechanism of the Gd-doped Sns is shown in Fig. 1(j).

The optical absorption of the synthesized pure and doped SnS nanoparticles was recorded was in the wavelength range of 200–800 nm with the help of UV–visible spectra as shown in Fig. 2. In these spectra, the exact optical absorption edge could not be seen. Hence, it was not possible to determine the optical band gap value for the synthesized samples. However, with the aid of the optical absorption data, the Tauc plot was used to calculate the $\alpha hc/\lambda_{ab}$ and $(\alpha hc/\lambda_{ab})^2$. This plot helps to find an accurate optical band of the synthesized samples. The optical band energy values are noted from the Tauc plot and are 1.65, 1.12 and 1.06 eV for pure SnS, Nd-doped SnS and Gd doped SnS nanostructures respectively. On introducing the dopant into the SnS material; the optical band gap values decreased. The reason for the decreasing optical band gap of the doped samples was the additional energy level between the valence band and conduction band of SnS.

When a magnetic field was applied in the positive and negative direction on the X-axis of the synthesized samples using the VSM instrument, the synthesized samples got magnetized and served to obtain the M−H loop (Fig. 3). From the M−H loop, could be detected the magnetic parameters, like the magnetic nature, intensity of magnetization, coercivity and retentivity values. A tiny hysteresis curve with a weak ferromagnetism could be seen for the pure SnS material in the M−H loop. However, the Nd and Gd doped SnS samples also showed a ferromagnetism nature, but for the hysteresis loop slight variations were observed compared to the pure SnS. This may be due to the rare earth metal ions Nd and Gd exchanging with the Sn ion, when the magnetic field was applied and as a consequence magnetic moment variation happened. The magnetic parameters of the pure and doped SnS nanostructures are shown in Table.1. Table.1 shows all the synthesized samples exhibiting the dilute magnetic semiconductors' characteristic nature. This was because the synthesized SnS samples have low coercivity values. Hence, the above magnetic parameters would be suitable for spintonic device applications.

The XRD patterns of the Gd doped SnS sample were taken and the above sample diffraction peaks' position and their corresponding diffraction planes were indexed, as shown in Fig. 4. The diffraction peaks of the synthesized SnS sample compared with the reported JCPDS No (39-0354) of the SnS material obtain from the XRD patterns, prove that the SnS sample reveals the formation of an orthrhombic phase structure [5]. The well defined peaks indicate that the synthesized Gd doped SnS has a good crystalline nature.

The antimicrobial activity of undoped-SnS, Nd-doped SnS and Gd-doped SnS against *E. coli* were shown in Fig. 5 (a-c). Gentamicin (+) and distilled water (-) were taken as the positive and negative controls respectively. The diameter of the zone of inhibition of the antibiotic was measured as 3.3 ± 0.2 cm. There was no zone of inhibition formed in the undoped-SnS and Nd-doped SnS samples whereas, in the Gd-doped SnS, the diameter of zone of inhibition was measured as 2.1 ± 0.2 cm. The Gd doped SnS nanoparticles exhibited the antimicrobial activity [51,52]. Gd^{3+} trivalent ions doped SnS material interact with the negative cell wall of the bacteria and damage it resulting in the leakage of cells. Further, the Gd ions doped SnS enter the bacterial cell and interrupt the production of nucleic acids. The increase in the reduced oxidative stress happened due to the disturbance in the protein synthesis [51,52]. Therefore ultimately, this results in the destruction of the bacteria.

4. Conclusion

In this investigation, three different materials like undoped SnS, Nd-doped SnS and Gd-doped SnS material have been synthesized using the . hydrothemal method. Their optical absorption, optical band gap, magnetic nature, coercivity, and magnetic saturation and zone of inhibition

values are compared and discussed in the results and discussion section. Based on the UV, VSM and antibacterial characterization, it is seen that relatively better optical, magnetic and antibacterial properties are found in Gd- doped SnS nanostructures compared to other undoped and Nd-doped SnS materials.

CRediT authorship contribution statement

J. Gajendiran: Methodology, Investigation, Writing – original draft, Writing – review & editing, Conceptualization, Validation. **S. Gnanam:** Investigation, Writing – original draft, Writing – review & editing. **V.P. Senthil:** Formal analysis. **J. Ramana Ramya:** . **K. Ramachandran:** . **V. Vijayakumar:** . **S. Gokul Raj:** Formal analysis. **G. Ramesh Kumar:** Conceptualization. **N. Sivakumar:** Formal analysis.

Declaration of Competing Interest

The authors declare that they have no known competing financial interests or personal relationships that could have appeared to influence the work reported in this paper.

References

[1] H. Tian, C. Fan, G. Liu, S. Yuan, Y. Zhang, M. Wang, E. Li, Appl. Surf. Sci. 487 (2019) 1043–1048.
[2] S.S. Hegde, B.S. Surendr, Vijaya Talapatadur, Prashantha Murahari, K. Ramesh, Chemical Physics Letters 754 (2020) 137665.
[3] A.M. Mostafa, E.A. Mwafyc, M.S. Hasanind, Opt. Laser Technol. 121 (2020) 105824.
[4] Y.T. Ma, J. Shuyi Ma, Z.G. Tang, J. Wu, Y. Shi, S.T. Zhao, P.F.C. Pei, Vacuum 181 (2020) 109657.
[5] Shujaat Ali, Fengping Wang, M. Zubair Iqbal, Hidayat Ullah Shah, Saba Zafar, Materials Letters 206 (2017) 22–25.
[6] K. Santhosh Kumar, C. Manoharan, S. Dhanapandian, A. Gowri Manohari, T. Mahalingam, Optik 125 (2014) 3996–4000.
[7] H. Kafashan, Ceram. Int. 45 (2019) 334345.
[8] F. Jamali-Sheini, M. Cheraghizade, R. Yousefi, Solid State Sci. 79 (2018) 30–37.
[9] S.H. Chaki, M.D. Chaudhary, M.P. Deshpande, Mater. Res. Bull. 63 (2015) 173–180.
[10] B. Parveen, M. Hassan, S. Riaz, S. Atiq, S. Naseem, M. Irfan, M.F. Iqbal, J. Magn. Magn. Mater. 460 (2018) 111–119.
[11] M. Reghima, A. Akkari, C. Guasch, M. Castagné, N. Kamoun-Turki, J. Renewable Sustainable Energy 5 (2013) 063109.
[12] P. Cermak, J. Hejtmanek, T. Plechacek, J. Navratil, J. Kasparov, V. Holý, Z. Zmrhalov, M. Jarosov, L. Benes, C. Drasar, J. Alloy. Compd. 811 (2019) 151902.
[13] A. Urbaniaka, M. Pawłowskia, M. Marzantowicza, B. Maríb, T. Sallb, Thin Solid Films 664 (2018) 60–65.
[14] K. Santhosh Kumar, C. Manoharan, S. Dhanapandian, A. Gowri Manohari, Spectrochim. Acta Part A Mol. Biomol. Spectrosc. 115 (2013) 840–844.
[15] H. Kafashan, Mater. Sci. Semicond. Process. 88 (2018) 148–160.
[16] H. Kafashan, M. Azizieh, Z. Balak, Appl. Surf. Sci. 410 (2017) 186–195.
[17] Mark Seal, Nirala Singh, Eric W. McFarl , Jonas Baltrusaitis, Journal of Physical Chemistry C 119, (12) (2015) 6471-6480.
[18] Prasert Sinsermsuksakul, Rupak Chakraborty, Sang Bok Kim, Steven M. Heald, Tonio Buonassisi, Roy G. Gordon, Chemistry of Materials. 24 (2012) 4556-4562.
[19] Z. Xiao, F.-Y. Ran, H. Hosono, T. Kamiya, Appl. Phys. Lett. 106 (2015) 152103.
[20] D. Trbojevic, P.M. Nikolic, B. Perovic, V. Cvekic, Appl. Phys. Lett. 38 (1981) 362.
[21] G.G. Ninan, V.G. Rajeshmon, C. Sudha Kartha, K.P. Vijayakumar, AIP Conf. Proc. 1591 (2014) 1440.
[22] Seyedeh Laleh Mousavi, Farid Jamali-Sheini, Mohammad Sabaeian, Ramin Yousefi, J. Phys. Chem. C 125 (2021) 15841–15852.
[23] Vera Steinmann, Riley E. Brandt, Rupak Chakraborty, R. Jaramillo, Matthew Young, Benjamin K. Ofori-Okai, Chuanxi Yang, Alex Polizzotti, Keith A. Nelson, Roy G. Gordon, Tonio Buonassisi, APL Materials 4 (2016) 026103.
[24] R. Hu, K. Zhu, K. Ye, J. Yan, Q. Wang, D. Cao, G. Wang, Appl. Surf. Sci. 536 (2021) 147832.
[25] S. Mei, W. An, J. Fu, W. Guo, X. Feng, X. Li, B. Gao, X. Zhang, K. Huo, Paul K. Chu, Electrochim. Acta 331 (2020) 135292.
[26] Y.T. Ma, S.Y. Ma, J. Tang, Z.G. Wu, J. Shi, Y. Zhao, S.T. Pei, Mater. Sci. Eng., B 263 (2021) 114861.
[27] H. Sun, S.J. Park, Appl. Surf. Sci. 531 (2020) 147325.
[28] B.K. Pandey, Ram Gopal, Mater. Lett. 272 (2020) 127842.
[29] Vinaya Kumar Arepalli, Sung Jun Kim, Jeha Kim, Journal of Physics and Chemistry of Solids 155 (2021) 110099.
[30] V.P. Jethwa, V.M. Kunjal Patel, G.K.S. Pathak, J. Alloy. Compd. 883 (2021) 160941.
[31] Purusottam Reddy Bommi reddy, Chandra Sekhar Musalikunta, Chalapathi Uppala, Si-Hyun Park, Materials Science in Semiconductor Processing 71 (2017) 139-144.
[32] Y. Qin, X. Wang, Physica E 131 (2021) 114752.
[33] V. Janakiramana, V. Tamilnayagam, R.S. Sundararajan, S. Sivabalan, B. Sathyaseelan, Chalcogenide Letters 17 (2020) 405–410.
[34] B. Parveen, M. Hassan, S. Atiq, S. Riaz, S. Naseem, M. Asif Toseef, Progr. Nat. Sci.: Mater. Int. 27 (2017) 303–310.
[35] M.P.A. Muthalif, Y. Choe, Appl. Surf. Sci. 508 (2020) 145297.
[36] K. Santhosh Kumar, A.Gowri Manohari, S. Dhanapandian, T. Mahalingam, Mater. Lett. 131 (2014) 167-170.
[37] Mohammad Reza Arefi-Rad, Hosein Kafashan, Opt. Mater. 105 (2020) 109887.
[38] A. Sobhani, M. Salavati-Niasari, Mater. Res. Bull. 47 (2012) 1905–1911.
[39] A. Sobhani, M. Salavati-Niasari, J. Mater. Sci. 26 (2015) 6831–6836.
[40] A. Sobhani, M. Salavati-Niasari, J. Mater. Sci.: Mater. Electron. 27 (2016) 293–303.
[41] M. Salavati-Niasari, A. Sobhani, H. Temp, Mater. Proc. 31 (2012) 157–162.
[42] A. Sobhani, M. Salavati-Niasari, Transition metal selenides and diselenides: Advances in Colloid and Interface Science. 287 (2021) 102321.
[43] A. Sobhani, M. Salavati-Niasari, J. Nanostruct. 7 (2017) 141–146.
[44] A. Sobhani, M. Salavati-Niasari, J. Mol. Liq. 220 (2016) 334–338.
[45] A. Sobhani, M. Salavati-Niasari, High Temp. Mater. Processes (London) 31 (6) (2012) 711–771.
[46] H. El-Saied, A.M. Mostafa, M.S. Hasanin, E.A. Mwafy, A.A. Mohammed, J. King Saud University-Sci. 32 (1) (2020) 436–442.
[47] E.A. Mwafy, M.S. Hasanin, A.M. Mostafa, Opt. Laser Technol. 120 (2019) 105744.
[48] A.M. Mostafa, E.A. Mwafy, J. Mol. Struct. 1222 (2020) 128913.
[49] A.M. Mostafa, E.A. Mwafy, E. Nanotechnology, Monitoring & Management 14 (2020) 100382.
[50] F.S. Alamro, A. Toghan, H.A. Ahmed, A.M. Mostafa, A.I. Alakhras, E.A. Mwafy, Microscopy Res. Technique (2021).
[51] P.SK. Aashima, S. Singh, S.K. Mehta, J. Colloid Interface Sci. 529 (2018) 496–504.
[52] S.M. Hunagund, V.R. Desai, D.A. Barretto, M.S. Pujar, J.S. Kadadevarmath, S. Vootla, A.H. Sidarai, J. Photochem. Photobiol., A 346 (2017) 159–167.